Engineered 3D-Vessels-on-Chip to study effects of dynamic fluid flow on human induced pluripotent stem cell derived endothelial cells

Graaf, M.N.S. de

Citation

Graaf, M. N. S. de. (2023, April 6). *Engineered 3D-Vessels-on-Chip to study effects of dynamic fluid flow on human induced pluripotent stem cell derived endothelial cells*. Retrieved from https://hdl.handle.net/1887/3590465

Version:	Publisher's Version
License:	Licence agreement concerning inclusion of doctoral thesis in the Institutional Repository of the University of Leiden
Downloaded from:	https://hdl.handle.net/1887/3590465

Note: To cite this publication please use the final published version (if applicable).

Chapter two:

Scalable Microphysiological System to Model Three-Dimensional Blood Vessels

Mees N. S. de Graaf[1], Amy Cochrane[1], Francijna E. van den Hil[1], Wesley Buijsman[2,3], Andries D. van der Meer[2], Albert van den Berg[3], Christine L. Mummery[1,2], Valeria V. Orlova[1]

[1] Department of Anatomy and Embryology, Leiden University Medical Center
[2] Applied Stem Cell Technologies, University of Twente
[3] BIOS Lab on a Chip, University of Twente

Published in APL Bioengineering 3, 026105 (2019); https://doi.org/10.1063/1.5090986

Abstract

Blood vessel models are increasingly recognized as having value in understanding disease and drug discovery. However, continued improvements are required to more accurately reflect human vessel physiology. Realistic three-dimensional (3D) in vitro cultures of human vascular cells inside microfluidic chips, or vessels-on-chips (VoC), could contribute to this since they can recapitulate aspects of the in vivo microenvironment by including mechanical stimuli such as shear stress. Here, we used human induced pluripotent stem cells as a source of endothelial cells (hiPSC-ECs), in combination with a technique called viscous finger patterning (VFP) towards this goal. We optimised VFP to create hollow structures in collagen I extracellular-matrix inside microfluidic chips. Lumen formation success rate was over 90% and the resulting cellularized lumens had a consistent diameter over their full length, averaging 336 ± 15 µm. Importantly, hiPSC-ECs cultured in these 3D microphysiological systems formed stable and viable vascular structures within 48 hours. Furthermore, this system could support co-culture of hiPSC-ECs with primary human brain vascular pericytes (HBVPs), demonstrating their ability to accommodate biologically relevant combinations of multiple vascular cell types. Our protocol for VFP is more robust than previously published methods with respect to success rates and reproducibility of diameter between- and within channels. This, in combination with the ease of preparation, makes hiPSC-EC based VoC a low-cost platform for future studies in personalised disease modelling.

2.1 Introduction

Blood vessels are lined with endothelial cells (ECs) and surrounded by mural cells called smooth muscle cells or pericytes. The interaction between mural cells and ECs provides many vessels with stability and abnormal interactions can lead to conditions such as haemorrhage, vascular dementia and chronic infection[1–3]. Furthermore, EC and mural cell interaction influences the selectivity of the barrier, which determines whether compounds can enter or are excluded from an organ, and they are therefore important factors in drug efficacy and tissue selectivity[4,5]. Studying interaction between ECs and mural cells can be complex; for instance, combining three-dimensional (3D) geometry and controlled fluid flow is challenging *in vitro*. Pseudo-capillary vascular networks can be generated when culturing vascular cells in conventional two-dimensional (2D) tissue culture plastic dishes but these lack the lumen of vasculature *in vivo*[6,7]. By contrast, ECs can self-organize in 3D culture environments into complex vascular capillary networks in which a perfusable lumen develops with diameters ranging from approximately 10 μm (the size of an *in vivo* capillary) to 100 μm[8]. However, precise control of the network geometry during self-organization is challenging and this creates intrinsic variation in wall shear stress when fluid flow is introduced. Wall shear stress is an important determinant of vascular function[9]. Its magnitude can be estimated by assuming blood vessels are straight cylinders with a constant flow rate and viscosity, using the following equation [8,10]:

$$\tau = \frac{32\,\mu\,Q}{\pi\,d^3} \qquad (1)$$

(Where τ: shear stress [Pa], μ: viscosity of the fluid [Pa * s], Q: flow rate [m^3/s], d: diameter [m])

In order to generate 3D vessels as experimentally tractable models with controlled geometries, techniques other than self-organization are necessary. Microphysiological systems (MPS) have been reported in which vascular cells are cultured in large-diameter, patterned 3D lumen inside a microfluidic chip[11]. These MPS are also referred to as 'vessel-on-chip' (VoC) systems. Many different engineering techniques are being developed to produce more complex MPS. Most often, VoCs are fabricated by patterning an extracellular matrix with a small-diameter needle[12,13]. This method yields reproducible lumens using straightforward methodology but scaling up of experiments is labour intensive and removing the template without disturbing the structure is challenging. An alternative method is viscous finger patterning (VFP). VFP is a microfluidic technique that exploits the difference in viscosity between two fluids to generate a scaffold that can be used for cell culture[14–16]. When a less viscous fluid displaces a viscous fluid in a confined channel, the less viscous fluid flows in a "finger-like" shape through the middle of the channel; this is referred to as the Saffman-Taylor finger (Figure 1b*i-iii*)[17]. When the viscous fluid is a soluble hydrogel that can gelate, this results in a hollow

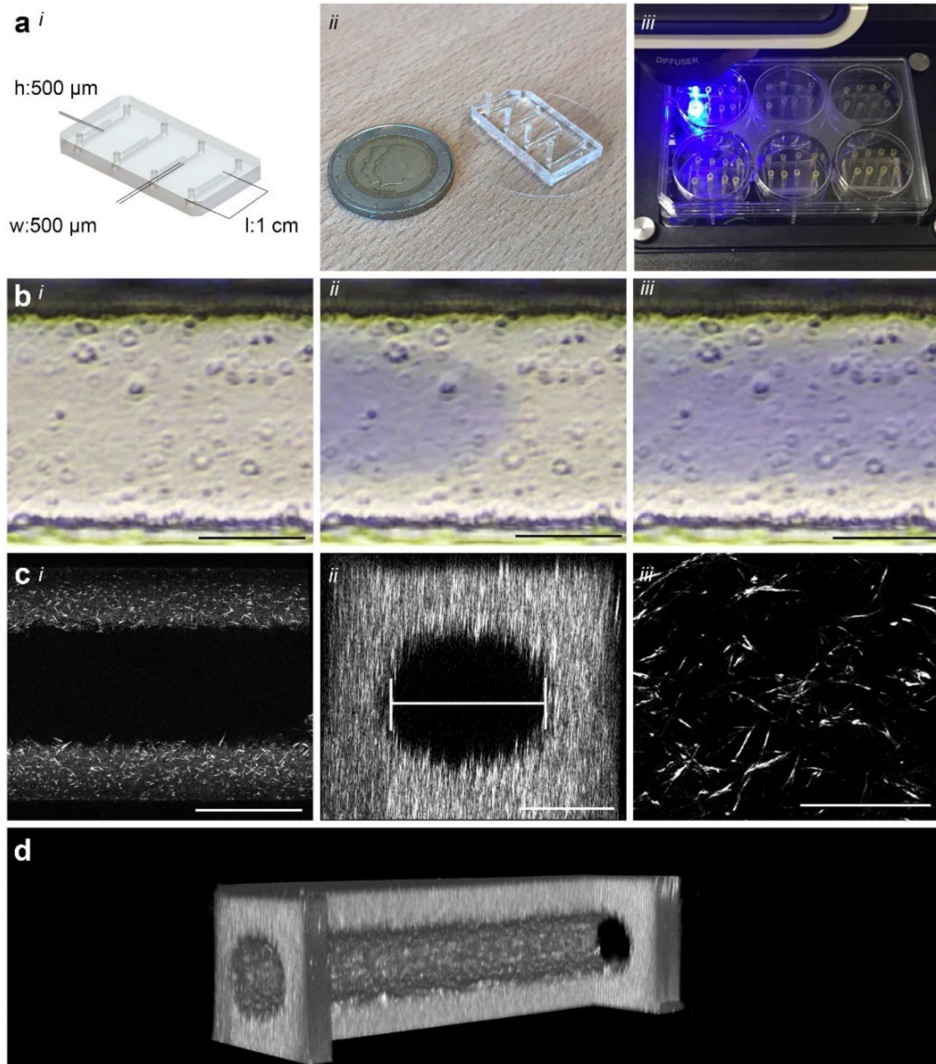

Figure 1: Microfluidic design and patterning collagen scaffold. (a). (i) *Schematic of the microfluidic chip showing dimensions and layout of the microfluidic platform, four straight channels on a single chip with designed parameters 500 µm × 500 µm × 1 cm (w×h×l)* ***(ii)*** *Photograph of the real microfluidic device showing four channels ready to be patterned, two-euro coin as size reference* ***(iii)*** *Photograph demonstrating ease of use and medium throughput capacity of this setup. The microfluidic device fits in 6-well plates allowing analyses medium throughput in a conventional biological workflow. Manual preparation of patterning of these 24 lumens is typically 10 minutes.* ***(b)*** *Time-lapse of Viscous finger patterning images showing PBS with blue food dye travelling through collagen solution in a 500 µm wide channel* ***(i)*** *t=0 collagen is injected* ***(ii)*** *PBS finger travels through the channel* ***(iii)*** *PBS-finger has completely traversed the channel and displaced the centre of the collagen (c) (i) 20x magnification confocal slice of a patterned lumen with 5 mg/ml collagen I; note the absence of fibril structure in the centre where the "finger" displaced the collagen.* ***(ii)*** *XZ- reconstruction showing the flow field of the scaffold. Diameter is determined by the widest slice of a reconstructed image****(iii)*** *63x magnification showing a detailed view of the fibril structure of collagen I* ***(d)*** *3D cut-out reconstruction of a 2-photon second harmonic generation image showing the collagen scaffold. One side has been cut out to demonstrate the inside of the scaffold.*

structure resembling a lumen. The width of the Saffmann-Taylor finger is approximately half of the channel width and height assuming sufficient difference in viscosity, no interface tension and sufficient velocity[18]. However, in practice, the dimensions achieved by several groups is approximately 60-80% of the channel dimensions[14,16]. A major benefit of VFP is that it can be easily scaled up as it only requires pipetting two fluids in a microfluidic channel. A downside of VFP to fabricate VoC systems is that the procedure to form the lumen is sensitive to many factors, such as extracellular matrix concentration and pH, timing, pressure and inlet and outlet geometries. Fabrication of VoC systems can thus be challenging and inherently variable.

Besides the method of fabrication, the biological aspect also needs to be considered. Typically, *in vitro* models incorporate primary human cells[6]. Although these cells are widely available from commercial sources or can be isolated directly from various human tissues, their supply is finite since they are not immortal. In addition, they exhibit donor-to-donor variability. This can negatively affect reproducibility and robustness of *in vitro* models. Human induced pluripotent stem cells (hiPSCs) can be used to generate vascular cells through differentiation with high reproducibility and robustness and therefore could improve cell quality and sustainability of VoC systems by allowing repeated return to the same (cryopreserved) singe cell source[19–21]. hiPSCs are derived by reprogramming somatic cells to a pluripotent state using four transcription factors: c-myc, Sox 2, Oct4, Klf4[22]. hiPSCs can be differentiated to all cells of the body including vascular cells if provided with the right growth factors. We have developed methods which support differentiation of ECs from hiPSCs (hiPSC-ECs) under defined culture conditions and have shown that these cells are functional in a multiplicity of assays *in vivo* and *in vitro*[23,24]. hiPSCs can be derived from patients with specific disease genotypes or healthy control individuals with minimally invasive tissue collection[25]. Furthermore, hiPSCs allow generation of cell types that are typically difficult to harvest from patients, like neurons from the brain or cardiomyocytes from the heart. Using advanced genetic modification, molecular indicators and markers can be introduced for live cell imaging and analysis[26]. Using the same techniques, isogenic healthy control hiPSC lines can be derived by genetic repair of the disease-causing mutation, minimizing differences and allowing effects of the mutation of interest to be studied independent of genetic background.

Here, we describe a robust and reproducible method to generate VoC systems using an optimized VFP protocol for dynamic flow experiments. We use hiPSC-ECs, rather than those isolated from primary tissues or blood from donors, to allow the inclusion of genetically marked cells into the device so that they can be precisely tracked. The system we describe represents an important advance in the fabrication of robust, low-cost VoC systems that will enable future dynamic studies in disease modelling and drug development.

2.2 Results

To optimise the VFP-technique, straight flow channels with fixed dimensions of 500 µm × 500 µm × 1 cm (w × h × l, Figure 1a*i*)) were designed to facilitate lumen formation. Master-moulds were fabricated with SU-8 photolithography to produce flow channels that were

highly similar. Polydimethylsiloxane (PDMS) casting of the master-moulds was used to fabricate chips by conventional soft lithography. Analysis of the PDMS cast showed that, on average, channels had a width of 496 ± 3.7 µm and height of 527 ± 1.2 µm, an aspect ratio of 1.06 (data not shown).

First, lumens were patterned as described by Bischel et al. with a minor modification (protocol 1: passive pumping (PP), Figure S1)[14]. This method relies on medium flow driven by the differential surface tension of a small droplet placed on the inlet and a large droplet on the outlet of the microfluidic channel. When the droplet on the outlet is sufficiently large, the force generated by passive pumping can be calculated using the following equation [2][27]

$$\Delta \mathrm{P} = \frac{2\gamma}{r} \qquad (2)$$

(where P: pressure [Pa], γ: surface tension [N/m], r: radius curvature of droplet [m])

This shows that a smaller initial droplet (i.e. higher curvature) generates more force. This curvature depends on the dimensions of the inlet, volume of the applied droplet and hydrophobicity of the surface. Patterned collagen I was imaged using two-photon second harmonic generation (2P-SHG, Figure 1c,d) and the diameter was analysed. The diameter was defined as the widest part of the reconstructed flow area (Figure 1c*ii*). In our hands, the protocol had a success rate (defined as generation of a perfusable lumen with the diameter <400 µm) of 90-100% depending on the operator. When comparing lumen diameter in the middle section of the flow channel, we observed that the average lumen diameter was 261 ± 28 µm, which is similar to that reported by others previously with comparable flow channel dimensions (cf 256 ± 21 µm) [15]. However, the analysis showed a significant entry effect so that these lumens gradually decreased in diameter over the length of the channel (Figure 2a*i* and 2b, blue line). Diameter analysis showed high inter-lumen variation, with diameters ranging from 220-320 µm (Fig 2d and Figure S3). We further observed additional variation when this protocol was performed by different operators. Interestingly, we observed that the lumen diameter was typically the smallest at around 5-7 mm from the inlet (Figure 2b).

We next patterned lumens by applying a modified protocol described by Herland et al. [16]; which relies on hydrostatic pressure on the chip inlets to drive lumen formation. As reported previously and from our experience, air-

bubbles were the major cause of failure with this protocol (data not shown). We therefore modified the protocol by introducing an additional step that included inserting an empty pipette tip prior to injecting the collagen (protocol 2: gravity driven (GD), Figure S1b). This allowed addition of PBS to the top of the collagen without introducing air bubbles. Lumens were imaged with 2p-SHG and the diameters measured (Figure 2a*ii* and 2b, orange line and Figure S4). Interestingly, the lumens patterned following this adaption showed a uniform diameter at the beginning of the channel, with gradual widening of the lumen at the end (Figure 2a*ii* and 2b, orange line). The GD protocol had a high success rate (defined as perfusable lumen with a diameter <400 μm) and improved intra-lumen diameter profile (Figure 2c); however, with the parameters used, this protocol was sensitive to small deviations in the volume and the height resulting in relatively high inter-lumen variation (Figure 2d). We also noticed that the GD protocol failed with some batches of collagen possibly due to batch-to-batch differences. To successfully initiate patterning with these collagen batches, more pressure was required (i.e. more driver fluid) which resulted in a widening of the lumen like that reported by Herland et al.

In order to generate uniform lumens with more pressure and less volume, we combined the protocols for passive pumping and extension of the pathway. To consistently extend the pathway, pipette tips were cut using a customized mould that resulted in uniform end lengths of 7 mm (protocol 3: extended passive pumping (EPP), Figure S1a). Lumens were imaged with 2P-SHG and the diameter measured (Figure 2a*iii* and 2b, grey line and Figure S4). Diameters typically showed a small oscillating trend around the average diameter across the average width of 255 ±12 μm (Figure 2d, Figure S4). Levene's statistical test showed non-equal variance ($p=0.007$), confirming smaller variance in diameter of lumens patterned using the EPP protocol (protocol 3) than the lumens patterned using the PP or GD protocols (protocol 1 and protocol 2 respectively). length of the channel. All lumens ($n=10$) had similar diameters with an As expected, one-way ANOVA analysis indicated no differences between the means ($p=0.654$). In higher throughput

of 3D vessels generated using the optimized EPP protocol. The flow profile was determined by the assessment of the velocity of the fluorescent beads that were perfused at a specific flow rate (20 μl/min).

Distances travelled by individual beads were manually measured at the specific segments of the channel to reconstitute the flow profile (Figure 5a,b). Shear stress was calculated from maximum velocity and diameter at the specific segments of the channel (Figure 5c, N=1). The cultured lumen was segmented into three Regions of Interest (ROI 1-3) and the average diameter was determined. ROI (ROI 1:320 μm, ROI2:290 μm ROI3: 300 μm) Flow profile analyses showed that on average the flow rates are comparable with

each other and the set flow rate (ROI 1: 18.8 ± 1.3 µl/min, ROI 2: 17.8 ± 1.5 µl/min, ROI 3: 18.0 ± 0.6 µl/min (cf set flowrate: 20 µl/min). The corresponding shear stress was calculated using equation 1. This analysis showed that, on average, shear stress was 0.27 Pa with a maximum of 13 % deviation within the ROIs thus validating the channels as being capable of producing equal sheer stresses along their length.

2.3 Discussion

To generate robust *in vitro* 3D vascular models, it is essential to balance bioengineering with cell biology; cell survival and functionality must be compatible with scaffold design. An important feature for high-utility technology is that it yields technical replicates regardless of operator. Currently, 3D vessels are fabricated by encapsulating and removing a small-diameter needle or PDMS rods in an extracellular matrix [12,29–32]. Although this method is straightforward and reproducible, it is laborious and difficult to scale up. To address this, we investigated the VFP the described by Beebe et al and showed it to be easily implementable and scalable but we observed gradual narrowing of the patterned lumen along its length. This change in lumen shape is a challenge in the context of dynamic studies since the ECs are subject to significantly different shear stresses when exposed to flow (up to 3-fold in a single channel). Shear stress has a pivotal role in cell fate and behaviour and intra-lumen variation would reduce the uniformity of results *a priori* in a single channel and require elaborate downstream analyses to interpret results. Diameter variation should therefore be kept to a minimum[10,33]. In this study we showed that by modifying the existing protocol by extending the entry length, we could rapidly generate reproducible 3D vascular structures with reduced variance without increasing difficulties in the technical preparation or requiring specialized equipment. The method proved to be scalable and typically 24 channels could be patterned by one person within 10 minutes. The protocol is low cost and can be easily implemented in a non-specialist biology lab. We further showed that these 3D vascular structures could support the culture of either hiPSC-ECs or cocultures of hiPSC-ECs and primary mural cells (HBVPs).

To generate circular lumens, we designed flow channels with a square cross-section. However, since manufacturing variability can be expected, dimensions were verified by analysing the cross-section of a PDMS cast. This showed that the resulting flow channel has a width approximately as designed (500 cf 496 µm). However, the height appeared to be consistently 529 µm, giving an aspect ratio (AR) of 1.06. It was therefore expected that the patterned lumens would also have an AR of 1.06.

In confocal microscopy, it is essential to use an immersion medium that exactly matches the refractive index of the sample to minimize differences in z-reconstruction[34]. The refraction index of a collagen I hydrogel has been

reported to be 1.336, close to that of water (1.333)[35]. However, depending on structure, concentration, and hydration this value variable, ranging from 1.3-1.5[36,37].

To investigate how this effect influences our diameter analyses, we imaged one lumen with three different immersion media. We observed that although the height was significantly affected by this refraction index mismatch, the width was not (Figure S6). Therefore, the diameter can be estimated by measuring the maximum width of a reconstructed lumen regardless of immersion medium or dry objectives. Dry objectives have major benefits in that they have typically longer working distance ranges and are able to switch to multiple fields during image acquisition, improving the throughput of confocal analyses.

As reported by Bischel et al., the diameter of the patterned lumen depends on the viscosity of the collagen, the velocity of patterning, and the dimensions of the microfluidic channel. The viscosity of collagen is highly dependent on its concentration[38]. Therefore, mixing a homogenous collagen solution is crucial for reproducibility between experiments. The stock solution of highly concentrated rat-tail collagen is extremely viscous and adhesive to standard pipette-tips and deviations were observed between different mixing batches. To optimize reproducibility between experiments, we found it best that the quantity of collagen be verified by weight and then diluted accordingly.

Furthermore, we observed during the throughput optimisation step that when many lumens were patterned from a single mixing batch, those last showed inconsistent lumen shapes. For this reason, we rigorously mixed the collagen, prepared it in small batches and used it immediately for optimal reproducibility. We observed that most lumens generated using protocol 1 tended to have a minimum diameter 5-7 mm from the inlet of the channel. By contrast, we observed a stable diameter at the beginning of the lumens patterned with protocol 2 and propose that extension of the pathway prior to the microfluidic channel could improve lumen diameter profile.

To extend the pathway, we inserted 7 mm cut pipette tips in the outlet prior patterning for three reasons. First, this prevents the narrowing of the patterned lumen near the inlet. By removing both pipette tips whilst twisting, the inlet and outlets are collagen-free allowing easy connection to a microfluidic flow system. Second, the shape of the driving droplet is not dependent on the hydrophobicity of the PDMS. The hydrophobicity of the microfluidic device changes after plasma treatment and surface functionalization and post-treatment, in a time-dependent manner and this introduces an extra variable[39]. By using an untreated, defined material, this hydrophobicity is constant and results in a constant driving force. Finally, patterning is less dependent on manufacturing errors like damaged or bent inlets by punching or casting variability. To cut these tips with a consistent

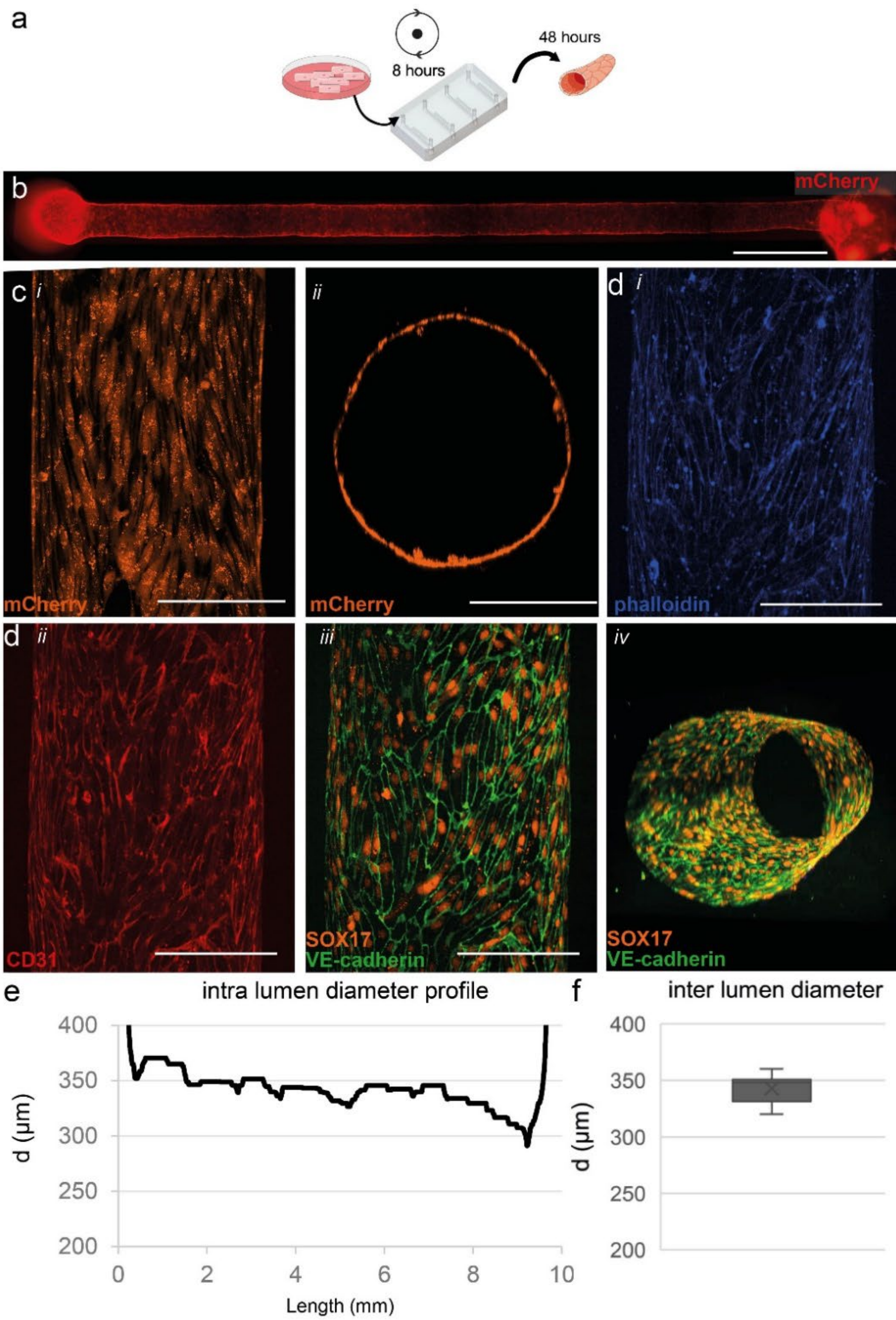
a
8 hours
48 hours
b
mCherry
c i
mCherry
ii
mCherry
d i
phalloidin
d ii
CD31
iii
SOX17
VE-cadherin
iv
SOX17
VE-cadherin
e
intra lumen diameter profile
d (µm)
Length (mm)
f
inter lumen diameter
d (µm)

length, we made a custom cutting guide. Using 3 mm and 5 mm extensions, we observed a distinct entry effect with a constriction at the inlet of the channel. Using the 7 mm extension this entry effect was reduced or vague.

It is important to use only straight cut tips of consistent length as an entry effect can be observed when tips are too short. To optimize the total length, we tested different tip lengths using the same diameter. Further extension could remove this entry effect completely, however required more collagen. Therefore, designated 7 mm as optimum. The patterned lumens are elastic and are significantly deformed by cell seeding during injection; however, we observed that this deformation is uniform and reproducible when similar pressures were applied during cell seeding experiments, the overall success was 88/96 (92%) of all attempts, defined as perfusable lumen with diameters <400 μm. while reducing the total length. These shortened tips were inserted such that their total height was respectively 3 mm, 5 mm and 7 mm from the coverslip. With the 3- and 5-mm extension, we observed an entry effect with a sudden decrease in diameter followed by a consistent diameter, similar to what was observed in the PP-protocol. With the 7 mm extension this effect was not observed or was less distinct (Figure S5).

The reason for failure was introduction of air bubbles that prevented patterning. To further optimize this protocol, we tested different path lengths to reduce total collagen volume. By first cutting a pipette tip at 7 mm and then shortening this small tip to 2 to 3 mm we kept the inlet diameter similar

In parallel, next to the patterning protocol, we also optimized cell seeding into the scaffolds. hiPSCs were genetically engineered to express the fluorescent protein mCherry ubiquitously and differentiated to ECs as described previously[23,24,28]. This allowed live cell imaging in 3D in real time. We tested various seeding densities (data not shown) and found that $1x10^7$ cells/ml was optimal for complete- and uniform channel coverage and high cell viability.

The microfluidic devices were slowly rotated for 8 hours to allow even cell attachment around the complete lumen (Figure 3a). After 48 hours, live cells

---

Figure 3: Three-dimensional cell culture of hiPSC-ECs. (a) *Schematic overview of cell seeding procedure and culture in microfluidic devices. hiPSC-ECs were seeded and cultured for 48 hours in static conditions.* ***(b)*** *Widefield image shows an even and consistent mCherry signal demonstrating uniform coverage of hiPSC-ECs along the whole lumen in a collagen scaffold.* ***(c) (i)*** *Top-down view of live cell confocal image* ***(ii)*** *XY-reconstruction of the live cell confocal microscopy confirms complete coverage around the perimeter of the lumen* ***(d)*** *Top-down reconstruction of the lumen visualised using the following markers* ***(i)*** *F-actin (phalloidin, visualised in blue)* ***(ii)*** *CD31 (visualised in red) and* ***(iii)*** *VE-Cadherin (visualised in green) at the periphery of the hiPSC-ECs co-stained with SOX17 (visualised in orange) localised at the nuclei of endothelial cells showing alignment with the longitudinal axis of the lumen* ***(iv)*** *3D reconstruction of the engineered vessel showing VE-cadherin and SOX17 around the complete periphery of the lumen and a more detailed reconstruction is presented in videoS1* ***(e)*** *Analyses of the full-length channel shows a uniform diameter with small tapering near the outlet* ***(f)*** *Diameter analysis of cellularized lumens (n=8), on average 343 ± 12 μm. Scale bars, b: 1000 μm, c, d: 200 μm*

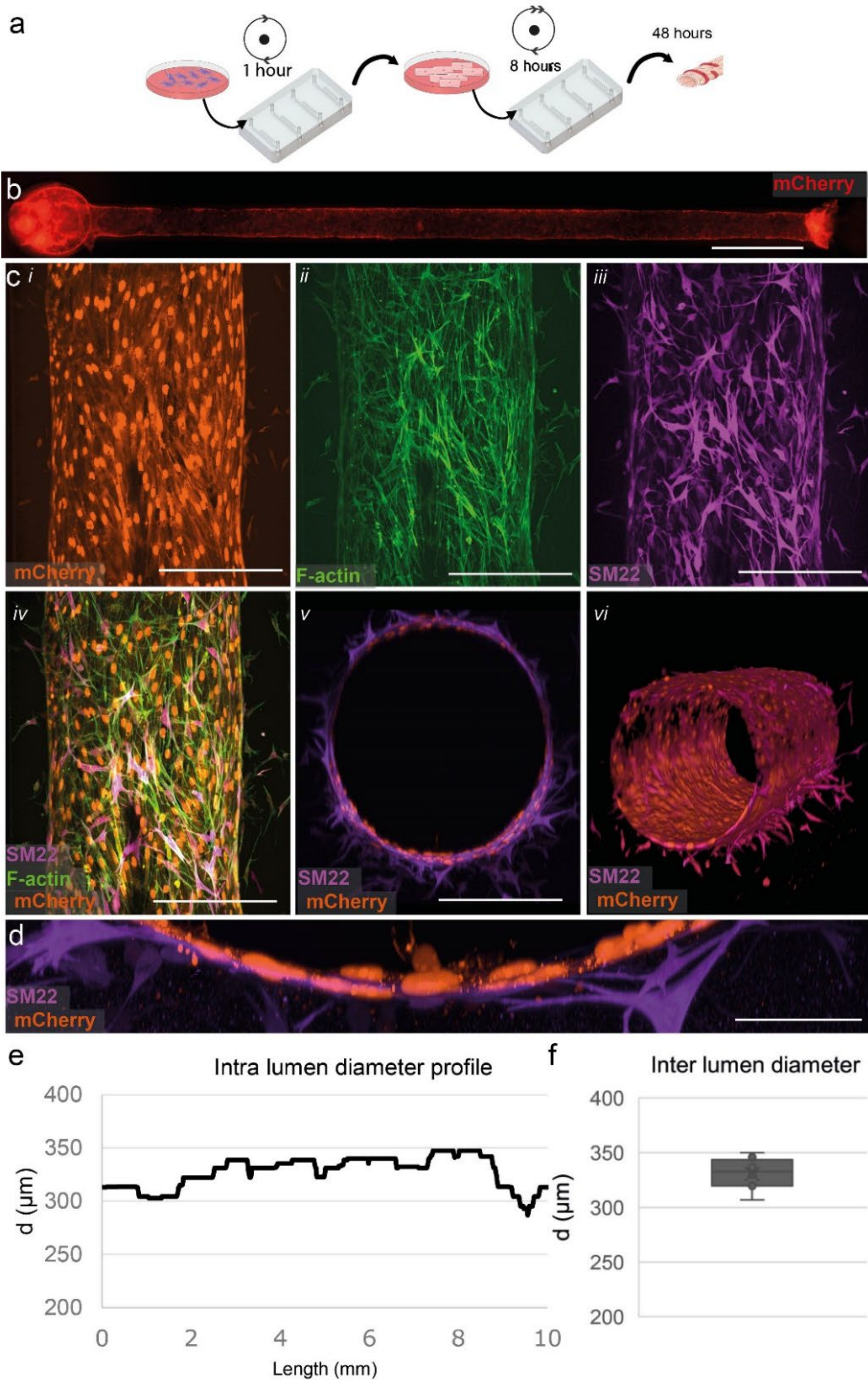
a
1 hour
8 hours
48 hours
b
mCherry
c i
ii
iii
mCherry
F-actin
SM22
iv
v
vi
SM22
F-actin
mCherry
SM22
mCherry
SM22
mCherry
d
SM22
mCherry
e
Intra lumen diameter profile
d (µm)
400
350
300
250
200
0
2
4
6
8
10
Length (mm)
f
Inter lumen diameter
d (µm)
400
350
300
250
200

were imaged using an EVOS fluorescence microscope (Figure 3b*)*. Even distribution of fluorescence from the mCherry expressing ECs was observed across the entire length of each channel. Further analyses using confocal fluorescence microscopy confirmed even coverage around the perimeter of the lumen (Figure 3c*i* and c*ii*). Analysis of the vessel diameter (n=8) showed an average width of 343 ± 12 µm (Figure 3f). The diameter profile was essentially uniform but was on average significantly wider than bare collagen lumens. VoCs were fixed and immunostained for the endothelial-specific markers CD31, SOX17 and VE-cadherin (Figure 3d). VE-cadherin was observed at the cell-cell junctions of the ECs, demonstrating uniform EC interaction and monolayer formation(Figure 3d*iii*).

To further recapitulate the architecture of *in vivo* vasculature, we generated 3D vessels with supporting mural cells (Figure 4). First, we seeded primary human brain vascular pericytes (HBVPs) into the lumen scaffold and rotated for 1 hour (Figure 4a). Next, hiPSC-ECs were seeded as described before and cultured for 48 hours. Uniform coverage by hiPSC-ECs was observed across the entire length of the scaffold similar to the monoculture (Figure 4b). HBVPs were also found evenly distributed across the microfluidic channel. This was evident in immunofluorescence images taken using spinning disk confocal microscopy which showed a uniform endothelial cell layer with adjacent mural cells, as visualized by mCherry (hiPSC-ECs), F-actin (hiPSC-ECs and HBVPs) and SM22 (mural cell-specific marker to label HBVPs) (Figure 4c*i*-*vi*, Supplementary Video). Notably, close interaction was observed between the HBVPs and hiPSC-ECs (Figure 4d). Importantly, measurement of the diameter of these vessels in the cocultures was comparable to that in the monocultures 331 ± 13 µm (n=8, non-significant p value= 0.18, Figure 4f). Typically, the diameter profile of the co-cultures shows a similar uniform expansion. To further explore the applicability of the technology in functional studies, such a shear-stress analysis and modelling endothelial-leukocyte interaction under flow, we determined the flow profile across the entire length of the channel It is important to point out that introduction of air bubbles severely deform the patterned lumens and must be avoided. This stable diameter ensured more

---

Figure 4: Three-dimensional coculture of hiPSC-ECs and HBVPs. (a) *Schematic overview of the protocol for cell seeding and culture in microfluidic devices.* ***(b)*** *Widefield image shows an even and consistent mCherry signal demonstrating uniform coverage of hiPSC-ECs along the whole lumen in collagen gel, similar to that of the monoculture* ***(c)*** *Top-down view of immunofluorescent staining showing close interaction of EC and pericytes* ***(i)*** *mCherry expressing ECs (visualized in orange)* ***(ii)*** *f-actin (visualised in green)* ***(iii)*** *SM22 staining HBVPs (visualized in magenta) and* ***(iv)*** *merged image of EC- and SMC- markers. (v) XZ-view demonstrating lumen lined with mCherry labelled ECs (orange) surrounded by HBVPs (magenta).* ***(vi)*** *3D reconstruction of the vascular tube, a complete reconstruction is presented in video S2.* ***(d)*** *High magnification of cross section, demonstrating close interaction between the inner EC-layer and surrounding HBVP supporting cells.* ***(e)*** *Diameter analyses of a full-length channel show uniform channel similar to monoculture.* ***(f)*** *Diameter analysis of the cellularized channel, on average 331 ± 13 µm (n=8).Scalebars, b: 1000 µm, c: 200 µm, d: 50 µm.*

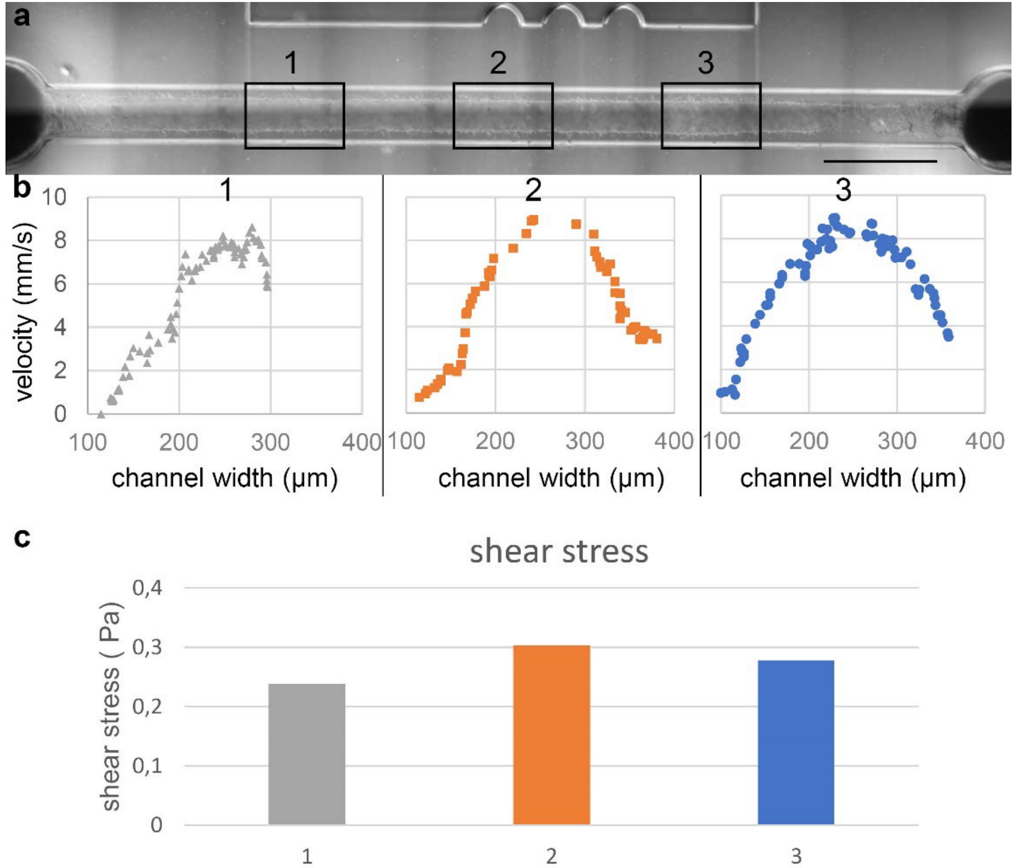

Figure 5: Analysis of the flow profile. (a) *Widefield image of the perfused lumen. Boxes are showing the pre-determined regions of interest (ROI) at 2.5 mm, 5 mm and 7.5 mm from the inlet. The average diameter of ROI 1; 320 µm, ROI 2: 290 µm, ROI 3, 300 µm. A full impression of the perfused lumen is presented in video S3.* ***(b)*** *Velocity profile reconstructed of 30 frames per ROI showing maximum velocity in the centre of the lumen. Some interaction of the beads with the cell wall can be observed. Using maximum velocity and assuming laminar flow the volumetric flow rate is determined to be respectively 19 µm/min, 18 µm/min, 18 µm/min.* ***(c)*** *Calculated shear stress per ROI using the determined flow rates and measure diameters. ROI 1 0.24 Pa, ROI 2: 0.30 Pa and ROI 0.28 Pa.*

uniform physiological conditions for cells seeded in the lumen, as evidenced by particle image velocimetry, allowing more accurate dynamic experiments to be performed. ~0.3 Pa is a physiologically low shear stress; however, with our current system, higher velocities could not be measured as the individual particles were not detected in two successive frames.

2.4 Conclusion and Future outlook

Lumens patterned using our protocol with standardized parameters resulted in high reproducibility in the fabrication of VoC systems without specialized structures consisting of hiPSCs-derived vascular cells. Furthermore, these vascular models were perfusable with minimal variation in shear stress. This

will eventually allow isogenic cells to be cultured as 3D vessels *in vitro* that recapitulate *in vivo* architecture. Combination of vascular and inflammatory cell types differentiated from hiPSCs may help to determine which cellular component of the vessel wall is affected by (genetic) disease and cause the disease phenotype. This platform was demonstrated to be fully compatible with various microscopes in conventional biological workflow. While we used straight channels here, the protocol is easily adapted to curved channels with similar results (Figure S7). This can be relevant for some pathologies that equipment. It also proved to be rapidly scalable and applicable to vascular result in different fluid mechanical conditions, such as atherosclerotic plaques in blood vessels, and could be modelled with this adaptable protocol.

2.5 Acknowledgments

Dr. Konstantinos Anastassiadis of the TU Dresden for kindly providing the following constructs: pPB-CAG-mCherry and pCMV-hyPBASE. The authors acknowledge the funding received from the Dutch Science Foundation (NWO) under the Gravitation Grant 'NOCI' Program (Grant no. 024.003.001) and this project has received funding from the European Union's Horizon 2020 research and innovation program under the Marie Sklodowska Curie grant agreement No. 707404.

2.6 Materials and Methods

Generation of mCherry expressing hiPSC line

NCRM-1 hiPSC line was obtained from RUDCR Infinite Biologics at Rutgers University (originally generated by NIH Center for Regenerative Medicine (NIH CRM)), additional information available in public database: https://hpscreg.eu/cell-line/CRMi003-A. Ethics approval is not required. The NCRM-1 line is a male control reference line obtained from CD34+ cord blood cells and is reprogrammed with an episomal plasmid. The cell line was modified in-house with a mCherry expression cassette under a CMV early enhancer/chicken β actin (CAG) promoter using a previously established protocol[40].

Differentiation hiPSC-ECs

hiPSC-ECs were differentiated using a previous protocol with minor modifications[23,28]. Briefly, hiPSCs were maintained in TeSR™-E8™ medium on vitronectin-coated 6-well plates and seeded at day-1. Twenty-four hours after seeding E8 medium was replaced with B(P)EL medium supplemented with 8 μM CHIR. On the day -1, the medium was replaced with B(P)EL medium supplemented with 50 ng/ml VEGF (R&D systems) and 10 μM SB431542 (Tocris Bioscience) and refreshed on days 7-9. hiPSC-ECs were isolated on day 10 using CD31-Dynabeads™ (Invitrogen) as previously described[28]. hiPSC-ECs from cryo-preserved batches were used in all further experiments.

Thawing and expanding of hiPSC-ECs
hiPSC-ECs cells were thawed, resuspended in complete Endothelial cell serum-free medium (EC-SFM, Gibco, cat. no. 11111-044) and plated on a 0.1% gelatine-coated culture flask in complete EC-SFM, as previously described[28]. Cells were used for experiments when nearly confluent by visual inspection, typically at day 4. Cells were harvested using TrypLE™ according to the manufacturer's instruction. All hiPSC-ECs were used at passage #2.

Fabrication of microfluidic devices
Master-moulds for the microfluidic devices were designed in SolidWorks (Dassault Systèmes SolidWorks Corp.) and fabricated in a cleanroom by SU-8 photolithography at the University of Twente. Dimensions of flow channels were 1 cm × 500 µm × 500 µm (l × w × h, fig 1a*i*). To fabricate the microfluidic devices, Polydimethylsiloxane (PDMS, Sylgard 184, Dow Corning) base agent was mixed 10:1 with curing-agent and poured onto the master-mould to yield a PDMS slab with a thickness of approximately 5 mm. This thickness created a more stable platform for pipetting without deforming the channels by manual handling. The PDMS was degassed for one hour at room temperature under vacuum and cured at 75 °C for 180 minutes. After curing, the PDMS was cooled to room temperature and carefully peeled off. Inlet holes were punched with Uni-Core punch (1.2 mm, GE Healthcare) and the microfluidic chip was cut to fit the cover glass. Round cover glasses (#1.5, ⌀ 34 mm Thermo scientific) were spin-coated with 100 µl PDMS (5 seconds 1000 RPM, 30 seconds 4000RPM, PDMS prepared as described above). The spin-coated cover glass and the prepared microfluidic devices were air plasma treated (2 minutes, 50 mA at 20 Pa) and contact bonded. To functionalize PDMS to covalently bind collagen I and support the scaffold, a 2-step process was carried out immediately after contact bonding. 5 % (v/v) (3-Aminopropyl)-triethoxysilane (APTES, Sigma-Aldrich) was prepared fresh in distilled water (Gibco®), injected in the channels and incubated for 30 minutes at RT. Channels were thoroughly rinsed with absolute ethanol and dried using a nitrogen-gas flow. Channels were subsequently injected with 10%(v/v) Glutaraldehyde (Sigma-Aldrich, in dH_2O) and incubated at RT for 30 minutes. Channels were thoroughly rinsed with absolute ethanol, dried with a nitrogen gas flow and baked at 75 °C for at least 5 hours to evaporate any residual ethanol and glutaraldehyde. It is essential to remove any residual glutaraldehyde and ethanol as this will affect cell viability.

Preparation of collagen I solution
The preparation of collagen I is an important step for reproducible lumens. High concentration rat tail collagen I (Corning) was prepared to a final concentration of 5 mg/ml on ice. Briefly, a stock solution was prepared using M199 medium 10X (Gibco®), distilled water (Gibco®) and 1M sodium hydroxide according to the manufacturer's instructions. The appropriate amount of collagen I was pipetted in an empty vial using a positive

displacement-pipette and weighed to verify quantity. The proper amount of stock solution was added to the collagen and carefully mixed. pH was adjusted with sodium hydroxide by adding until the colour of the mixture changed from yellow to pink indicating a pH of approximately 7.4. The pH of collagen I is crucial for the mechanical properties; therefore care must be taken to perform this step as reproducibly as possible[41]. The collagen I mixture was always thoroughly mixed and spun down to remove air bubbles and kept on ice. Mixed collagen was used within 10 minutes.

Pattering of lumens using Viscous Finger Patterning

A schematic representation of all methods is given in Figure S1. The protocol as published by Bischel et al. was performed with a minor adaption as presented in Figure S1 protocol 1. To be able to connect the microfluidic devices to a microfluidic pump a large outlet port was not possible. For this reason, we left a pipette tip filled with collagen behind to reduce the surface tension. The protocol published by Herland et al. was modified to improve success-rate by inserting an empty pipette tip before injecting the collagen (Figure S1 protocol 2: GD). This allows applying the PBS to induce the needed hydrostatic pressure without a manual error.

Our protocol (Figure S1 protocol 3 EPP) is as follows. A standard P10 pipette tip (Greiner Bio-One #741015) was cut at approximately 7 mm from the tip using a custom fabricated cutting guide and inserted into the outlet of the microfluidic channel. 10 µl of collagen I mixture was injected via the inlet of the channel with a P10 pipette tip until the meniscus of the collagen I mixture reached the outlet of the microfluidic channel. The pipette tip was carefully and smoothly ejected from the pipette, keeping the meniscus at the outlet and leaving the pipette tip and the remaining collagen in the inlet. To achieve this, when attaching the pipette tip to the pipette, it is important to press only lightly to ensure a smooth release. Immediately, 3.5 µl of PBS was carefully pipetted on top of the collagen in the small tip to initiate patterning. Patterning typically takes 15 seconds and can be confirmed by disappearing of the applied droplet and a rise in the collagen level in the opposite tip. Alternatively, PBS can be supplemented with contrasting food dye for visual confirmation of patterning. However, this affects surface tension and requires an extra washing step before cell seeding as the compounds might influence cells or (fluorescent) microscopy. Immediately after patterning lumens, were incubated for 30 minutes at 37 °C in a humid incubator. After 30 minutes, EGM-2 medium (Lonza) was pipetted in the pipette tip and channels were incubated overnight at 37 °C to allow the pH to set. Prior to cell seeding, pipette tips were removed in a smooth twisting motion. To prevent the formation of air bubbles and deformation of the patterned collagen, the cut pipette tip was first removed and inserted a new pipette tip. The medium was then added to this pipette tip and the intact pipette tip removed. A new pipette

tip was then carefully inserted. These pipette-tips aids injecting cells into the channels and act as medium reservoirs.

Three-dimensional cell-culture

Primary human brain vascular pericytes (HBVP, ScienCell) were obtained and cultured in pericyte medium (ScienCell). Cells were harvest using TrypLE™, and resuspended at a concentration of $3.3x10^6$ cells/ml. 10 µl of cell suspension was carefully injected using gel loading pipette-tips. Care was given not to introduce any air-bubbles that might deform the collagen scaffold. This was achieved by generating a small droplet in the pipette-tip before inserting. The microfluidic device was put on a rotator (0.4 RPM, channel longitudinal axis in line with rotating axis) to allow even distribution of cells for 1 hour at 37 °C. hiPSC-ECs were harvested as described above and resuspended at a concentration of $1x10^7$ cells/ml. 5 µl of cell suspension was carefully injected using gel loading pipette-tips. The microfluidic device was put on a rotator (0.4 RPM, channel longitudinal axis in line with rotating axis) and slowly rotated for 8 hours at 37 °C to ensure complete coverage of the lumen. For monocultures, only ECs were seeded. Microfluidic devices were placed in a 6-well culture plate and incubated under static conditions at 37 °C. dH_2O was added between wells to prevent evaporation. Culture Medium (EGM-2+ pen/strep) was supplemented with VEGF (50 ng/ml) and refreshed every 24 hours.

Two-photon second harmonic generation

Unstained Collagen I was imaged using two-photon second harmonic generation (2P-SHG) with a Leica SP5 confocal microscope and a multi-photon laser tuned at 810 nm. Emitted light was detected with a BG38 band-pass filter (CWL 470) before the detector.

Flow profile analysis

Microfluidic channels were placed on a microscope and connected to a 1 ml syringe pump (Cole Palmer) using 45° 20g blunt needles. Culture medium was supplemented with 5 µm fluorescent beads and the flow rate was set to 20 µl/min. The flow was allowed to settle for 1 minute after which 30 frames per location were recorded at a pre-determined location (2.5 mm, 5 mm, 7.5 mm of the channel) at a frame rate of 30 frames per second. All frames were combined per location to reconstitute the flow profile and the maximum velocity was determined. The average diameter of the location was determined using a widefield image and the local shear stress was calculated using equation 1 using the calculated values assuming the viscosity of 37C medium reported as 0.0008[8].

Live cell imaging

Wide-field microscopy was performed using EVOS FL auto 2 microscope with a 4× (NA 0.4) air objective. Live cell confocal microscopy was performed using

a Leica SP5 inverted microscope using mCherry excitation/emission settings and a 20×(NA 0.75) water immersion objective.

Immunofluorescence staining
Cells were fixed by injecting 4 % PFA solution in the channels and incubated for 15 minutes at RT. Cells were subsequently permeabilised using 0.1 % (v/v) Triton-X 100 in PBS(-) for 10 minutes at RT. Channels were blocked with 1 % BSA in PBS(-) (w/w) for 30 minutes at RT. Primary antibodies were diluted (1:200) and injected into the channels and incubated overnight at 4 °C. Samples were rinsed three times with PBS(-). Secondary antibodies were diluted (1:300) in 1 % BSA and injected into the channels. Channels were incubated at RT for 1 hour and washed three times with PBS(-) for 10 minutes. DAPI was used to stain cell nuclei. After washing steps, pipette-tips were filled with PBS(-) to prevent drying out and were stored in the dark at 4 °C until imaging.

Fluorescence imaging
Immuno-stained cells were imaged using a Leica SP8 microscope equipped with a Dragonfly® spinning disk (Andor) using 20× (NA 0.75) water objective or 63× oil (NA 1.4).

Image handling
Images generated with the Leica SP5 were handled using Fiji ImageJ software. Images generated with the Leica SP8 spinning disk were handled with Imaris software (Bitplane, Oxford Instruments). For a top-down view, a full Z-stack was halved. A maximum projection of the halved stack was made to visualize the top monolayer.

Diameter analyses
In Fiji ImageJ Z-stacks were resliced with 10 µm spacing to XZ-view to visualize the formed lumen. For 2p-SHG, the stack was smoothed to reduce gaps and the average intensity and standard deviation inside the lumen were measured. A threshold value was calculated with the following equation:

$$\mathbf{Threshold} = \mathbf{Average\ mean} + \mathbf{3} \times \mathbf{Stdv} \quad (3)$$

The ImageJ magic wand-tool was programmed to trace the inner lining, and an ellipse was fitted. From the measurement, the width of the object was retrieved. Measurements under 100 µm and above 400 µm were excluded and replaced by an interpolated value. Full-length channels were plotted against the length. For inter lumen analyses, 1.5 mm around the centre of the channel was measured and the average diameter was taken as the diameter of that channel. Cell covered lumens were manually measured using an XZ-reconstruction and measured outside the mCherry signal. Results are shown as average diameter ± standard deviation.

Statistical analysis

Statistical analyses were performed with the IBM SPSS 25 software package. A Kolmogorov-Smirnoff test was performed to test for normal or uniform distribution. A test of homogeneity of variances (Levene's test) was performed to compare variances of the analysed diameters. One-way ANOVA test was performed to compare the means.

Supplementary materials

See supplementary material for a detailed overview of all viscous finger patterning protocols performed, 2P-SHG cross sections of all lumens analysed, representative diameter analyses of the pathway length optimisation and the XZ reconstruction and analyses of a lumen imaged using different immersion media. Supplementary videos of the 3d reconstruction of the monoculture and co-cultures and an example of the flow profile are also available.

References

1. Zhao, Z., Nelson, A. R., Betsholtz, C. & Zlokovic, B. V. Establishment and Dysfunction of the Blood-Brain Barrier. *Cell* **163,** 1064–1078 (2015).
2. Sweeney, M. D., Kisler, K., Montagne, A., Toga, A. W. & Zlokovic, B. V. The role of brain vasculature in neurodegenerative disorders. *Nat. Neurosci.* **21,** 1318–1331 (2018).
3. Storkebaum, E., Quaegebeur, A., Vikkula, M. & Carmeliet, P. Cerebrovascular disorders: Molecular insights and therapeutic opportunities. *Nat. Neurosci.* **14,** 1390–1397 (2011).
4. Daneman, R., Zhou, L., Kebede, A. A. & Barres, B. A. Pericytes are required for blood-brain barrier integrity during embryogenesis. *Nature* **468,** 562–566 (2010).
5. Stratman, A. N. *et al.* Interactions between mural cells and endothelial cells stabilize the developing zebrafish dorsal aorta. *Development* **144,** 115–127 (2017).
6. Sliwinska, P. N. *et al. Consensus guidelines for the use and interpretation of angiogenesis assays*. *Angiogenesis* doi:10.1007/s10456-018-9613-x
7. Simons, M. *et al. State-of-the-art methods for evaluation of angiogenesis and tissue vascularization: A scientific statement from The American Heart Association*. *Circulation Research* **116,** (2015).
8. Kim, S., Lee, H., Chung, M. & Jeon, N. L. Engineering of functional, perfusable 3D microvascular networks on a chip. *Lab Chip* **13,** 1489 (2013).
9. Baeyens, N. *et al.* Endothelial fluid shear stress sensing in vascular health and disease Find the latest version : Endothelial fluid shear stress sensing in vascular health and disease. **126,** 821–828 (2016).
10. Papaioannou, T. G. & Stefanadis, C. Vascular wall shear stress: basic principles and methods. *Hell. J. Cardiol.* **46,** 9–15 (2005).
11. Ingber, D. E. Reverse Engineering Human Pathophysiology with Organs-on-Chips. *Cell* **164,** 1105–1109 (2016).
12. José A. Jiménez-Torres, Stephen L. Peery, Kyung E. Sung, and D. J. B. LumeNEXT: A Practical Method to Pattern Luminal Structures in ECM Gels José. *Adv. Healthc. Mater.* **22,** 4311–4316 (2012).
13. Hasan, A., Paul, A., Memic, A. & Khademhosseini, A. A multilayered microfluidic blood vessel-like structure. *Biomed. Microdevices* **17,** 88 (2015).
14. Bischel, L. L., Lee, S.-H. & Beebe, D. J. A Practical Method for Patterning Lumens through ECM Hydrogels via Viscous Finger Patterning. *J lab Autom.* **17,** 96–103 (2012).
15. Lauren L. Bischel, Young, E. W. K., Mader, B. R. & Beebe, D. J. Tubeless Microfluidic Angiogenesis Assay With Three- Dimensional Endothelial-lined Microvessels. *Biomaterials* **25,** 1471–1477 (2013).
16. Herland, A. *et al.* Distinct contributions of astrocytes and pericytes to neuroinflammation identified in a 3D human blood-brain barrier on a chip. *PLoS One* **11,** 1–21 (2016).
17. P.G. Saffman & Taylor, G. I. The penetration of a fluid into a porous medium or Hele-Shaw cell containing a more viscous liquid. *Proc. Roy. Sot. A* **245,** 12–329, (1958).
18. Langaas, K. & Yeomans, J. M. Lattice Boltzmann simulation of a binary fluid with different phase viscosities and its application to fingering. *Eur. Phys. J. B* **141,** 133–141 (2000).
19. Kamm, R. D. *et al.* Perspective: The promise of multi-cellular engineered living systems. *APL Bioeng.* **2,** 040901 (2018).
20. Sinha, S. & Santoro, M. M. New models to study vascular mural cell embryonic origin: Implications in vascular diseases. *Cardiovasc. Res.* **114,** 481–491 (2018).
21. Lin, Y., Gil, C. H. & Yoder, M. C. Differentiation, evaluation, and application of human induced pluripotent stem cell?derived endothelial cells. *Arterioscler. Thromb. Vasc. Biol.* **37,** 2014–2025 (2017).
22. Takahashi, K. *et al.* Induction of Pluripotent Stem Cells from Adult Human Fibroblasts by Defined Factors. *Cell* **131,** 861–872 (2007).
23. Orlova, V. V. *et al.* Functionality of endothelial cells and pericytes from human pluripotent stem cells demonstrated in cultured vascular plexus and zebrafish xenografts. *Arterioscler. Thromb. Vasc. Biol.* **34,** 177–186 (2014).
24. Halaidych, O. V. *et al.* Inflammatory Responses and Barrier Function of Endothelial Cells Derived from Human Induced Pluripotent Stem Cells. *Stem Cell Reports* **10,** 1642–1656 (2018).
25. Raab, S., Klingenstein, M., Liebau, S. & Linta, L. A Comparative View on Human Somatic Cell Sources for iPSC Generation. *Stem Cells Int* **2014,** 768391 (2014).
26. Shinnawi, R. *et al.* Monitoring human-induced pluripotent stem cell-derived cardiomyocytes with genetically encoded calcium and voltage fluorescent reporters. *Stem Cell Reports* **5,** 582–596 (2015).
27. Walker, G. M. & Beebe, D. J. A passive pumping method for microfluidic devices. **V,** 131–134 (2002).

28. Orlova, V. V *et al.* Generation, expansion and functional analysis of endothelial cells and pericytes derived from human pluripotent stem cells. *Nat. Protoc.* **9,** 1514–1531 (2014).
29. Polacheck WJ, Kutys ML, Tefft JB, C. C. Microfabricated blood vessels for modeling the vascular transport barrier. *Nat. Protoc.* 1–32 (2019).
30. Polacheck WJ, Kutys ML, Yang J, Eyckmans J, Wu Y, Vasavada H, Hirschi KK, C. C. A non-canonical Notch complex regulates adherens junctions and vascular barrier function. *Nature* **552,** 258–262 (2017).
31. Ingram PN, Hind LE, Jiminez-Torres JA, Huttenlocher A, B. D. An Accessible Organotypic Microvessel Model Using iPSC-Derived Endothelium. *Adv Healthc. Mater* **7,** 1700497–10 (2017).
32. Wong AD, S. P. Live-cell imaging of invasion and intravasation in an artificial microvessel platform. *Cancer Res.* **74,** 4937–4945 (2014).
33. Baratchi, S. *et al.* Molecular Sensors of Blood Flow in Endothelial Cells. *Trends Mol. Med.* **23,** 850–868 (2017).
34. Besseling, T. H., Jose, J. & Blaaderen, A. Van. Methods to calibrate and scale axial distances in confocal microscopy as a function of refractive index. *J. Microsc.* **257,** 142–150 (2015).
35. Buchanan, C. F. *et al.* Three-dimensional microfluidic collagen hydrogels for investigating flow-mediated tumor-endothelial signaling and vascular organization. *Tissue Eng. Part C. Methods* **20,** 64–75 (2014).
36. Wang, X., Milner, T. E., Chang, M. C. & Nelson, J. S. Group refractive index measurement of dry and hydrated type I collagen films using optical low-coherence reflectometry. *J. Biomed. Opt.* **1,** 212–216 (1996).
37. Leonard, D. W. & Meek, K. M. Refractive indices of the collagen fibrils and extrafibrillar material of the corneal stroma. *Biophys. J.* **72,** 1382–1387 (1997).
38. Shayegan, M. & Forde, N. R. Microrheological Characterization of Collagen Systems: From Molecular Solutions to Fibrillar Gels. *PLoS One* **8,** 23–28 (2013).
39. Bodas, D. & Khan-malek, C. Hydrophilization and hydrophobic recovery of PDMS by oxygen plasma and chemical treatment — An SEM investigation. **123,** 368–373 (2007).
40. Rostovskaya, M. *et al.* Transposon-mediated BAC transgenesis in human ES cells. *Nucleic Acids Res.* **40,** (2012).
41. Raub, C. B. *et al.* Image correlation spectroscopy of multiphoton images correlates with collagen mechanical properties. *Biophys. J.* **94,** 2361–2373 (2008).

Chapter two: Supplementary Materials
Scalable microphysiological system to model three-dimensional blood

Electronic supplementary information and supplementary videos available at:

https://aip.scitation.org/doi/10.1063/1.5090986

Supplementary Methods

Refraction index mismatch analysis

To correctly reconstruct confocal images in 3D it is important to match the refraction index of the immersion medium with the sample. To investigate how this mismatch affects for our diameter analyses we analysed 3 different immersion media

A 3D co-culture was cultured, fixed and stained as described in methods. One lumen was subsequently imaged with a dry, water immersion and oil immersion objective (20x magnification NA 0.75, Figure S6a-c).

Pathway length optimization

Protocol 3 was modified to test different pathway lengths. Pipette tips were first cut to 7 mm as previously described. These tips were further reduced to approximately 2 to 3 mm. PDMS was cast on the master moulds 2.5 mm thick and the shortened tips were inserted in such way that the inlet was respectively 3 mm and 5 mm from the coverslip. From here all steps are described in the manuscript methods section, see “Pattering of lumens using Viscous Finger Patterning” and Figure S5.

Supplementary Figures and Table

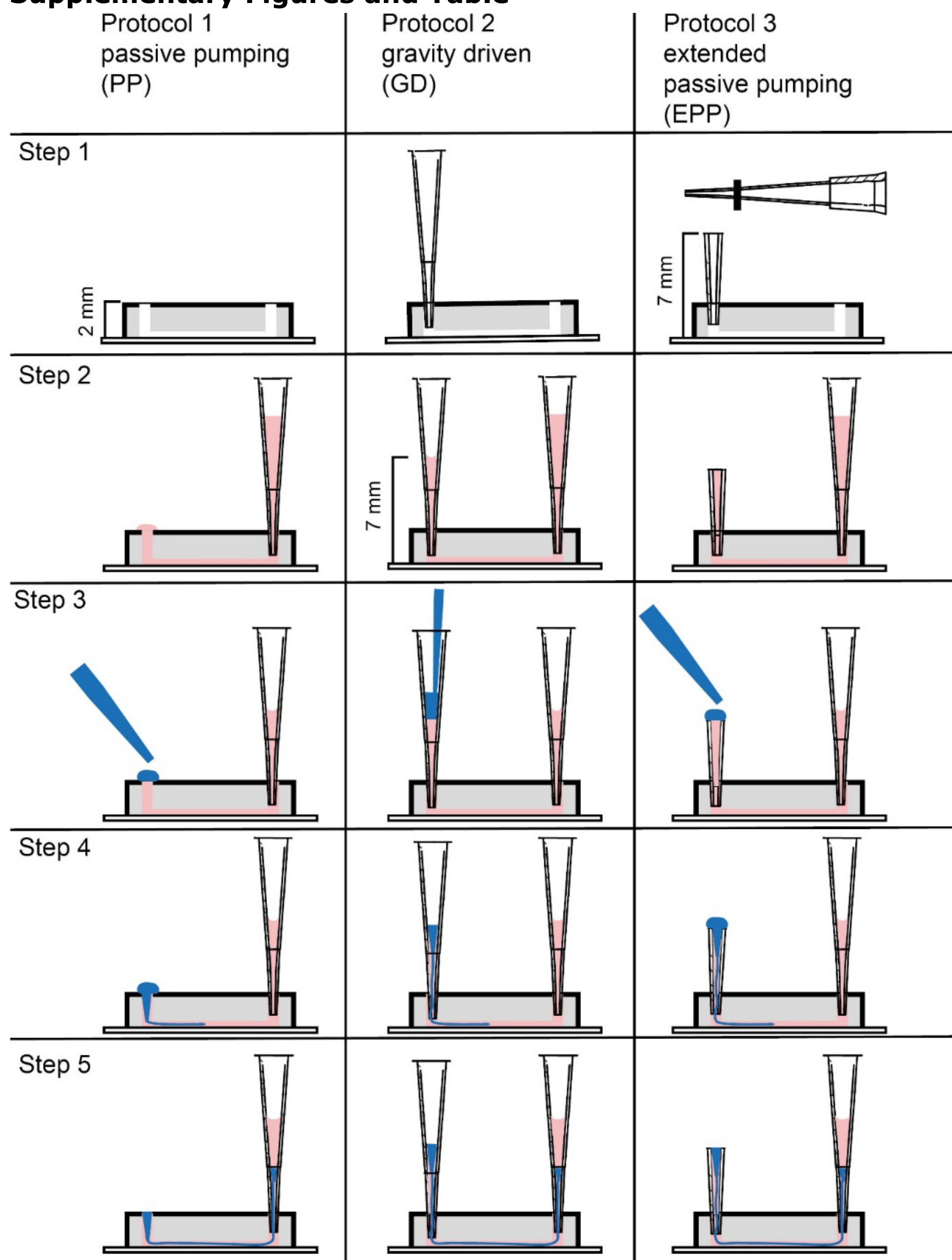

Figure S1: Schematic representation of the VFP protocols

Figure legend on next page

Protocol 1 passive pumping (PP) step 1 *preparation, PDMS was cast on the master moulds 2 mm thick and inlet holes were punched with an Uni-core 1.2 mm biopsy puncher (Harris), resulting in an 800 µm inlet/outlet hole;* ***step 2*** *collagen injection, a 5 mg/ml collagen I solution was mixed as described by Bischel et al. and carefully injected into the microfluidic channel until a meniscus formed on top of the outlet, then the pipette tip was carefully ejected, leaving the pipette tip and remaining collagen behind;* ***step 3*** *initiation, 2 µl of PBS was carefully placed on top of the collagen meniscus;* ***step 4*** *viscous finger patterning starts immediately after placement of droplet;* ***step 5*** *gelation, after the finger completely traversed the channel the microfluidic device is placed in a humid incubator at 37ºC to allow the collagen to gelate completely.*

Protocol 2 Gravity driven (GD) step 1 *preparation, PDMS was cast on the master moulds 3-5 mm thick and inlet holes were punched with a Uni-core 1.2 mm biopsy puncher (Harris), resulting in an 800 µm inlet/outlet hole. An empty Greiner Bio-One p10 pipette tip is placed in the outlet;* ***step 2*** *collagen injection, a 5 mg/ml collagen I solution was mixed as described in material and methods and carefully injected into the microfluidic channel until the meniscus reaches approximately 7 mm inside the pipette tip(first mark) on top of the outlet, then the pipette tip was carefully ejected from the pipette, leaving the pipette tip and remaining collagen behind;* ***step 3*** *initiation, 10 µl of PBS was carefully placed on top of the collagen meniscus;* ***step 4*** *viscous finger patterning starts immediately after placement of droplet;* ***step 5*** *gelation, after the finger completely traversed the channel the microfluidic device is placed in a humid incubator at 37ºC to allow the collagen to gelate completely.*

Protocol 3 Extended passive pumping (EPP) step 1 *preparation, PDMS was cast on the master moulds 3-5 mm thick and inlet holes were punched with a Uni-core 1.2 mm biopsy puncher (Harris), resulting in an 800 µm inlet/outlet hole. A Greiner Bio-One p10 pipette-tip is cut to approximately 7 mm from the tip using a cutting guide and inserted in the outlet;* ***step 2*** *collagen injection, a 5 mg/ml collagen I solution was mixed as described in material and methods and carefully injected into the microfluidic channel until a meniscus formed on top pipette tip of the outlet, then the pipette tip was carefully ejected from the pipette, leaving the pipette tip and remaining collagen behind;* ***step 3*** *initiation, 3.5 µl of PBS was carefully placed on top of the collagen meniscus;* ***step 4*** *viscous finger patterning starts immediately after placement of droplet;* ***step 5*** *gelation, after the finger completely traversed the channel the microfluidic device is placed in a humid incubator at 37ºC.*

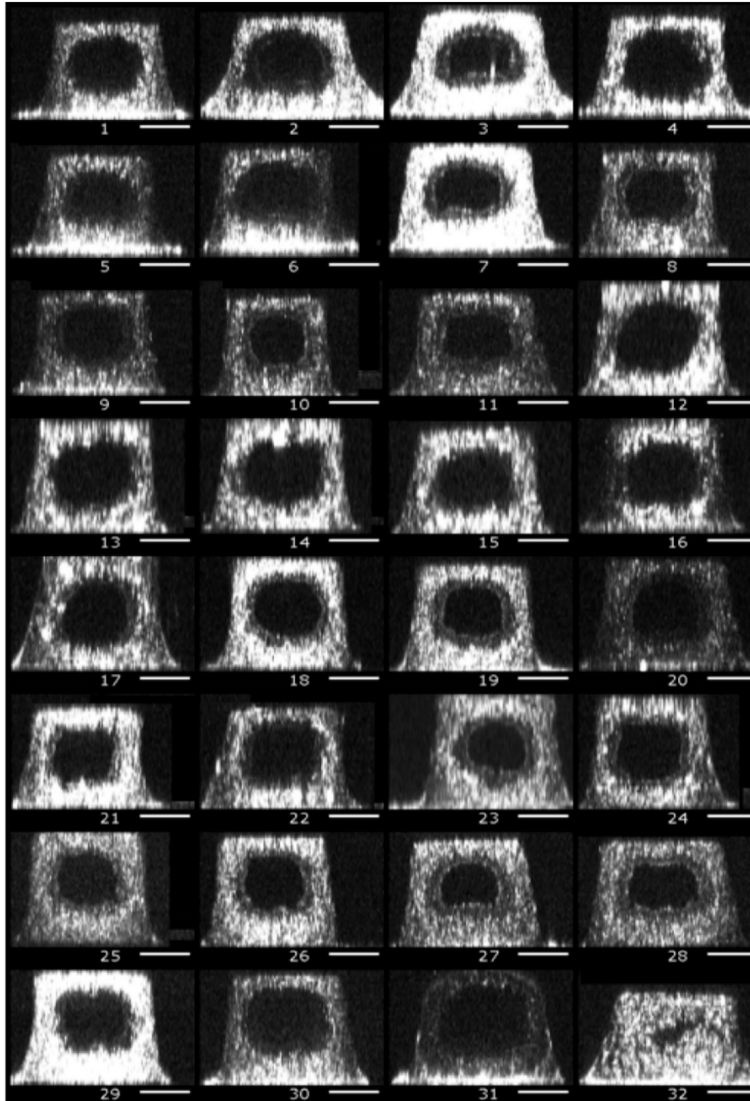

Figure S2: Cross sections of the PP lumens. *A cross-sectional view of the centre of all measured lumens patterned with protocol 1. Lumens were imaged using a 10x water objective. High variation in collagen structure, lumen shape and lumen diameter can be observed. The diameter was determined by the width of a fitted ellipse. All scale bars 200 µm.*

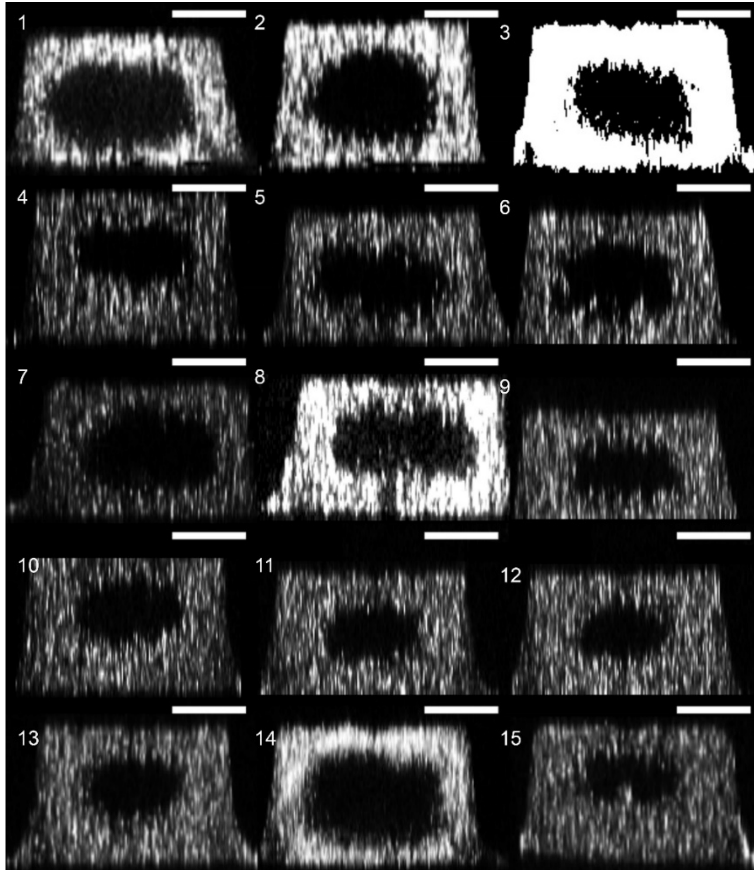

Figure S3: Cross sections of the GD lumens. *A cross-sectional view of the centre of all measured lumens patterned with protocol 2. Lumens were imaged with a 10x dry objective. collagen showed more uniform structures and shape was much more consistent. Still, high variation of lumen diameter was observed. The diameter was determined by the width of a fitted ellipse. All scale bars 200 μm.*

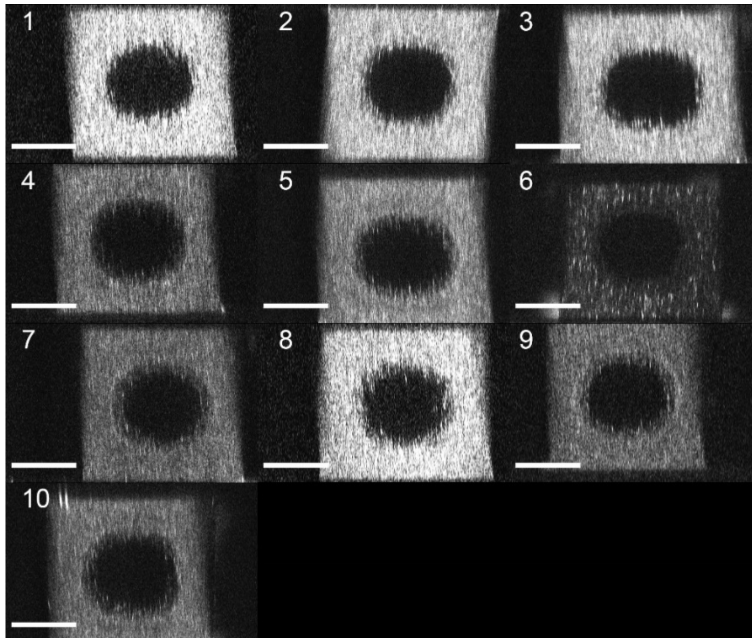

Figure S4: Cross sections of the EPP lumens. *A cross-sectional view of the centre of all measured lumens patterned with protocol 3. Lumens were imaged with a 20x water objective. Lumens show much more consistent collagen structure lumen shape and diameter. The diameter was determined by the width of a fitted ellipse. All scale bars 200 µm.*

a *i*

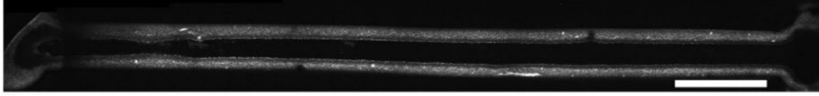

ii

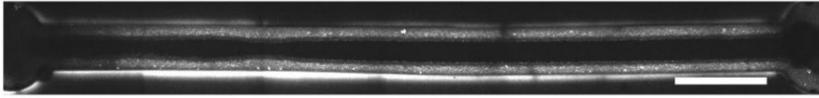

b

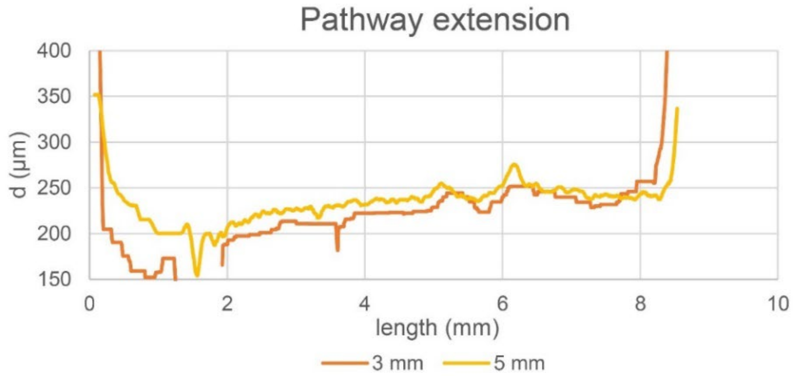

Figure S5 Path length optimization (a) A representative example of a lumen patterned with an extension of (i) 3 mm and (ii) 5 mm. **(b)** Diameter profile of a lumen patterned with an extension of 3 mm **(orange)** and 5 mm **(yellow)** show a significant entry effect as a sudden narrowing at the beginning of the channel.

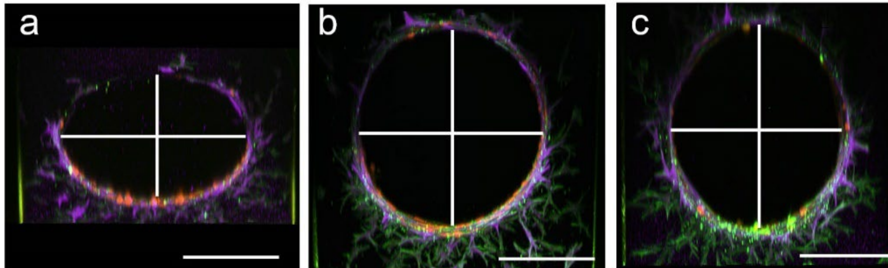

Figure S6: Analysis of the effect of refractive index mismatch. *The same lumen was imaged to investigate the height with three different 20x objectives:* ***(a)*** *dry objective, the reconstruction resulted in an elliptical flow area with a height of 236 µm (aspect ratio W/H, (AR:0.71);* ***(b)*** *water objective, the reconstruction resulted in a near circular flow area with a height of approximately 355 µm (AR:1.06);* ***(c)*** *oil objective resulted in an oval shape with a height of 378 µm (AR:1.12). Notably, the maximum widths of the lumens were all similar and therefore can be used for consequent and consistent diameter quantification regardless of used immersion media.*

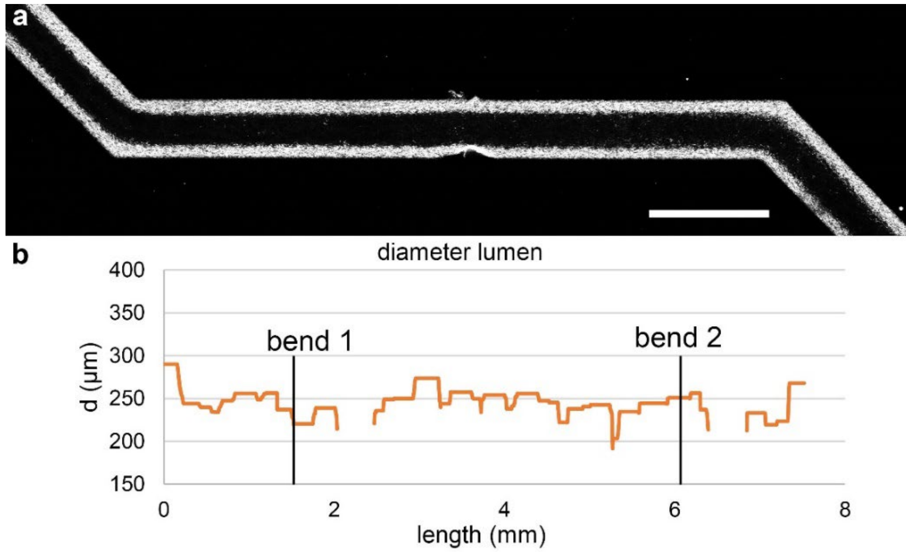

Figure S7: Example of a curved lumen.(a) *2P-SHG image of a double curved lumen in a 500 µm width channel;* ***(b)*** *Diameter profile of a double curved lumen showing that the lumen follows the channel with a minimal variation in diameter**.***

Table S1: Dimension analysis refractive index mismatch.

20x objective Immersion medium	Width (µm)	Height (µm)	Aspect ratio
Dry	343	236	0.69
Water	340	355	1.06
Oil	339	378	1.12